Arch Appl Mech (2010) 80: 353–376
DOI 10.1007/s00419-009-0321-2

ORIGINAL

Masoud Asgari · Mehdi Akhlaghi

Transient thermal stresses in two-dimensional functionally graded thick hollow cylinder with finite length

Received: 20 September 2008 / Accepted: 27 March 2009 / Published online: 12 April 2009

Abstract In this paper transient thermal stresses in a thick hollow cylinder with finite length made of two-dimensional functionally graded material (2D-FGM) based on classical theory of thermoelasticity are considered. The volume fraction distribution of materials, geometry and thermal load are assumed to be axisymmetric but not uniform along the axial direction. The finite element method with graded material properties within each element is used to model the structure. Temperature, displacements and stress distributions through the cylinder at different times are investigated. Also the effects of variation of material distribution in two radial and axial directions on the thermal stress distribution and time responses are studied. The achieved results show that using 2D-FGM leads to a more flexible design so that time responses of structure, maximum amplitude of stresses and uniformity of stress distributions can be modified to a required manner by selecting suitable material distribution profiles in two directions.

Keywords 2D-FGM · Finite length hollow cylinder · Transient thermal stress

1 Introduction

One of the engineers concern in designing structures under multi-functional requirements such as high temperature and large mechanical loads is the uniformity of stress distribution and the time response of structures. To this end composition of several different materials is often used in structural components in order to optimize the thermal and mechanical loadings responses in recent years. For reducing the local stress concentrations induced by abrupt transitions in material properties, the transition between different materials is made gradually. This idea was used by Japanese researchers firstly [1], leads to the concept of functionally graded materials. These materials are expected to be used for thermal applications and high rate thermal loading. In the application of FGM cylindrical structures to aerospace, nuclear and automobile industries, analysis of transient heat transfer and transient thermal stresses are of great importance. Analytical and computational studies of stresses, displacements and temperature in cylindrical shell made of FGM have been carried out by some of researchers.

Based on the multi-layered method, Kim and Noda [2] studied the unsteady-state thermal stress of FGM circular hollow cylinders by using of Green function method. Also a multi-layered material model was employed to solve the transient temperature field in a FGM strip with continuous and piecewise differentiable material properties by Jin [3]. Shao and Wang [4] considered analytical solution of transient thermo-mechanical stresses of FGM hollow cylinders were derived by using the Laplace transform technique and the power series method,

M. Asgari · M. Akhlaghi (✉)
Department of Mechanical Engineering, Amirkabir University of Technology,
P.O. Box 15875-4413, Hafez Ave., Tehran, Iran
E-mail: makhlagi@aut.ac.ir
Tel.: +98-21-64543409
Fax: +98-21-66419736

in which effects of material gradient and heat transfer coefficient on time-dependent thermal and mechanical stresses were discussed. Using finite difference method, Awaji and Sivakuman [5] studied the transient thermal stresses of a FGM hollow circular cylinder, which is cooled by surrounding medium. A long boundary integral equation method with the moving least squares approximation was applied to transient heat conduction analysis in functionally graded material by Sladek et al. [6]. Thermo-mechanical analysis of functionally graded hollow circular cylinders subjected to mechanical loads and linearly increasing boundary temperature is carried out by Shao and Ma [7]. Employing Laplace transform techniques and series solving method for ordinary differential equations, solutions for the time-dependent temperature and thermo-mechanical stresses are obtained in their study. The sensitivity analysis of heat conduction for functionally graded materials and the steady state and transient problem treated with the direct method and the adjoint method were presented by Chen et al. [8]. Transient temperature field and associated thermal stresses in FGM have been determined by using a finite element-finite difference method by Wang et al. [9]. A finite element-finite difference method was developed also to solve the time dependent temperature field in non-homogeneous materials such as FGMs by them [10]. Hosseini et al. [11] studied the transient heat conduction in functionally graded cylinder using an analytical method. They derived the temperature distribution by using Bessel functions. Shao [12] by using a multi-layered approach based on the theory of laminated composites presented the solutions of temperature, displacements, and thermal/mechanical stresses in a functionally graded circular hollow cylinder. The cylinder had finite length and was subjected to axisymmetric thermal and mechanical loads. The material properties are assumed to be temperature-independent and radially dependent, but were assumed to be homogeneous in each layer.

In most of the mentioned cases the volume fraction and properties of the FGMs are one-dimensional dependent and properties vary continuously from one surface to the other with a prescribed function while in advanced machine elements, temperature and load distributions may change in two or three directions [13]. Therefore, if the FGM has two-dimensional dependent material properties, more effective material resistance can be obtained. Based on this fact a two-dimensional functionally graded (2D-FGMs) whose material properties are bi-directionally dependent are introduced. Recently a few authors investigated 2D-FGMs. Aboudi et al. [14] studied thermo-elastic/plastic theory for the response of materials functionally graded in two directions. Cho and Ha [15] optimized the volume fraction distributions of 2D-FGM for relaxing the effective thermal stresses. Alla [13] investigated the reduction of thermal stresses by developing 2D-FGM materials. In that study a FGM plate under transient thermal loading was considered and finite element method had been used to solve the governing equations. There are numerous numerical methods to model the variation of material properties in FGMs. Conventional finite element formulations use a single material property to each element such that the property field is constant within an individual element. But using this method for transient and dynamic problems leads to significant discontinuities and inaccuracies. These inaccuracies will be more significant in 2D FGM cases. Sentare and Lambros [16] and Kim and Paulino [17] showed that graded finite elements can improve accuracy without increasing the number of degrees of freedom and decreasing the size of elements.

Analysis of transient thermal stresses of thick hollow cylinder with finite length made of 2D FGMs was not seen in the previous literature. In this paper, we consider a thick hollow cylinder with finite length made of 2D-FGM that its material properties are varied in the radial and axial directions with a power law function. The response of the structure under transient thermal load is considered. Also the thermoelectricity equations as well as heat transfer equations are developed in the both radial and axial directions. Variation of temperature and components of stresses with time as well as two-dimensional distributions of stresses and temperature through the cylinder in different times are analyzed. The volume fraction distribution, thermal load and cylinder geometry are assumed to be axisymmetric but not uniform along the axial directions. The effect of two-dimensional material distribution on the time response of the structure and stress distributions are studied. The finite element method with graded material properties within each element is used to model the material properties variations. Material properties are calculated by using linear rule of mixture and prescribed volume fraction in each point. The Crank–Nicolson method [18] is used to solve the governing equations of heat transfer problem in time domain.

2 Problem formulation

In this section volume fraction distribution in the two radial and axial directions is introduced. The governing equations of heat transfer and thermoelasticity in axisymmetric cylindrical coordinates are obtained and graded finite element is used for modeling the non-homogeneity of the materials.

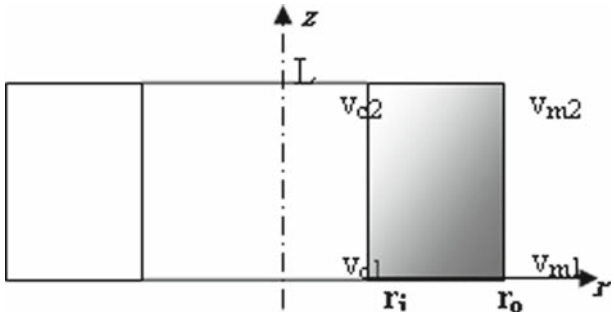

Fig. 1 Axisymmetric cylinder with two dimensional material distributions

2.1 Volume fraction and material distribution in 2D-FGM cylinder

Two-dimensional FGMs are usually made by continuous gradation of three or four distinct material phases that one or two of them is/are ceramics and the others are metal alloy phases. The volume fractions of the constituents vary in a predetermined composition profile. Now consider the volume fractions of a 2D-FGM at any arbitrary point in the 2D-FGM axisymmetric cylinder of internal radius r_i, external radius r_o, and finite length L shown in Fig. 1. In the present cylinder the inner surface is made of two distinct ceramics and the outer surface from two metals. $c1$, $c2$, $m1$ and $m2$ denote first ceramic, second ceramic, first metal and second metal, respectively.

The volume fraction of the first ceramic material is changed from 100% at the lower surface to zero at the upper surface by a power law function. And also this volume fraction is changed continuously from inner surface to the outer surface. The volume fractions of the other materials change similar to the mentioned one in two directions. The function of volume fraction distribution of each material can be explained as

$$V_{c1} = \left[1 - \left(\frac{r - r_i}{r_0 - r_i}\right)^{n_r}\right]\left[1 - \left(\frac{z}{L}\right)^{n_z}\right], \tag{1a}$$

$$V_{c2} = \left[1 - \left(\frac{r - r_i}{r_0 - r_i}\right)^{n_r}\right]\left[\left(\frac{z}{L}\right)^{n_z}\right], \tag{1b}$$

$$V_{m1} = \left(\frac{r - r_i}{r_0 - r_i}\right)^{n_r}\left[1 - \left(\frac{z}{L}\right)^{n_z}\right], \tag{1c}$$

$$V_{m2} = \left(\frac{r - r_i}{r_0 - r_i}\right)^{n_r}\left(\frac{z}{L}\right)^{n_z}, \tag{1d}$$

where subscripts $c1$, $c2$, $m1$ and $m2$ denote first ceramic, second ceramic, first metal and second metal, respectively. Also n_r and n_z are non-zero parameters that represent the basic constituent distributions in r and z directions. For instant, the volume fraction distributions of two basic materials for the typical values of $n_r = 2$ and $n_z = 3$ are shown in the Figs. 2 and 3. In this case $r_i = 1$ m, $r_o = 1.5$ m and $L = 1$ m.

Material properties at each point can be obtained by using the linear rule of mixtures, in which a material property, P, at any arbitrary point (r, z) in the 2D-FGM cylinder is determined by linear combination of volume fractions and material properties of the basic materials as

$$P = P_{c1}V_{c1} + P_{c2}V_{c2} + P_{m1}V_{m1} + P_{m2}V_{m2}. \tag{2}$$

The basic constituents of the 2D-FGM cylinder are presented in Table 1.

It should be noted that Poisson's ratio is assumed to be constant through the body. This assumption is reasonable because of the small differences between the Poisson's ratios of basic materials.

For instant, the variation of a material property such as specific heat capacity based on the mentioned approach through the cylinder, for the typical values of $n_r = 2$ and $n_z = 3$ is shown in Fig. 4.

2.2 Governing equations

Consider a 2D-FGM thick hollow cylinder of internal radius r_i, external radius r_o, and finite length L. Because of axisymmetric geometry and loading, cylindrical coordinates r and z are used in the analysis.

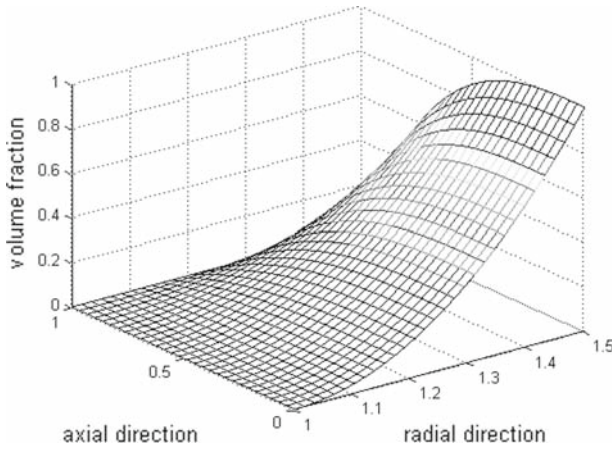

Fig. 2 Volume fraction distribution of $m1$

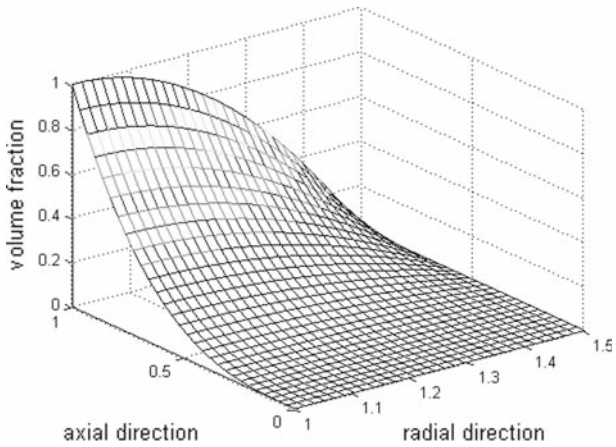

Fig. 3 Volume fraction distribution of $c2$

Table 1 Basic constituents of the 2D-FGM cylinder

Constituents	Material	E (Gpa)	ρ (kg/m^3)
$m1$	Ti6Al4V	115	4,515
$m2$	Al 1100	69	2,715
$c1$	SiC	440	3,210
$c2$	Al_2O_3	300	3,470

2.2.1 Heat transfer equations

Without the existence of heat sources, the equation of heat conduction in axisymmetric cylindrical coordinates is obtained as

$$1/r\frac{\partial}{\partial r}\left(rk_r(r,z)\frac{\partial T\,(r,z,t)}{\partial r}\right)+1/r\frac{\partial}{\partial z}\left(rk_z(r,z)\frac{\partial T\,(r,z,t)}{\partial z}\right)=\rho(r,z)c(r,z)\frac{\partial T\,(r,z,t)}{\partial t}, \qquad (3)$$

where $k_r(r,z)$, $k_z(r,z)$, $\rho(r,z)$ and $c(r,z)$ are thermal conductivity in the radial and axial directions, mass density and heat capacity of functionally graded material, respectively, that vary in two directions. The thermal conductivities in the radial and axial directions are assumed to be the same.

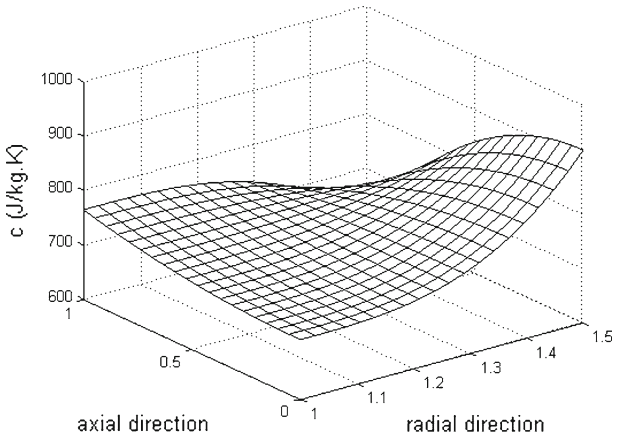

Fig. 4 Variation of specific heat capacity through the cylinder

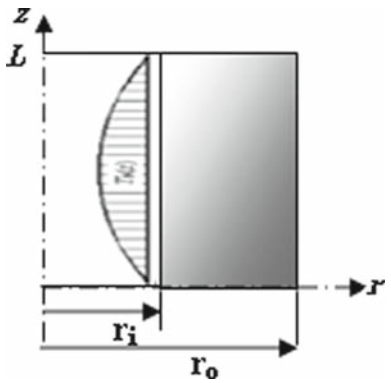

Fig. 5 Temperature distribution on the internal surface

The thermal boundary conditions are as follow:

$$\text{Temperature at inner radius:} \quad T(r_i, z, t) = T_i(z, t), \tag{4}$$

$$\text{heat convection at the outer radius:} \; k_r \frac{\partial T(r_o, z)}{\partial r} + h_o(T - T_\infty) = 0, \tag{5}$$

$$\text{heat convection at the lower edge:} \; k_z \frac{\partial T(r, 0)}{\partial z} + h_b(T - T_\infty) = 0, \tag{6}$$

$$\text{heat convection at the upper edge:} \; k_z \frac{\partial T(r, L)}{\partial z} + h_u(T - T_\infty) = 0, \tag{7}$$

where h_0, h_b and h_u are convection coefficients on the outer, lower and upper surfaces, respectively. T_∞ is the surrounding temperature and $T_i(z, t)$ is the thermal loading function for the internal surface expressed as

$$T(z, t) = f(t) \sin\left(\frac{\pi z}{L}\right), \tag{8}$$

in which

$$f(t) = T_c \left(1 - e^{c_0 t}\right), \tag{9}$$

where T_c and c_0 are constant values. The function $f(t)$ denotes variation of inner surface temperature with time.

An instantaneous temperature distribution on the internal surface is illustrated in Fig. 5.

The initial temperature of the cylinder is $T(r, z, 0) = T_o$.

2.2.2 Thermoelasticity equations

For evaluation of thermal stresses due to temperature gradient the classical thermoelasticity is used. Based on this theory the equilibrium and strain displacement equations are the same as elasticity problems.

Neglecting body forces the equilibrium equations are [19]:

$$\frac{\partial \sigma_{rr}}{\partial r} + \frac{\sigma_{rr} - \sigma_{\theta\theta}}{r} + \frac{\partial \tau_{rz}}{\partial z} = 0, \tag{10}$$

$$\frac{\partial \tau_{rz}}{\partial r} + \frac{\partial \sigma_{zz}}{\partial z} + \frac{\tau_{rz}}{r} = 0. \tag{11}$$

The strain-displacement relations are the same as that of homogeneous material as [19]

$$\varepsilon_{rr} = \frac{\partial u}{\partial r}, \tag{12a}$$

$$\varepsilon_{\theta\theta} = \frac{u}{r}, \tag{12b}$$

$$\varepsilon_{zz} = \frac{\partial w}{\partial z}, \tag{12c}$$

$$\gamma_{rz} = \frac{\partial u}{\partial z} + \frac{\partial w}{\partial r}. \tag{12d}$$

But constitutive stress–strain–temperature relations are

$$\sigma_{rr} = \frac{E(r,z)}{(1+\upsilon)(1-2\upsilon)}\left[(1-\upsilon)\varepsilon_{rr} + \upsilon(\varepsilon_{\theta\theta} + \varepsilon_{zz})\right] - \frac{E(r,z)\alpha(r,z)}{1-2\upsilon}T(r,z), \tag{13a}$$

$$\sigma_{\theta\theta} = \frac{E(r,z)}{(1+\upsilon)(1-2\upsilon)}\left[(1-\upsilon)\varepsilon_{\theta\theta} + \upsilon(\varepsilon_{rr} + \varepsilon_{zz})\right] - \frac{E(r,z)\alpha(r,z)}{1-2\upsilon}T(r,z), \tag{13b}$$

$$\sigma_{zz} = \frac{E(r,z)}{(1+\upsilon)(1-2\upsilon)}\left[(1-\upsilon)\varepsilon_{zz} + \upsilon(\varepsilon_{rr} + \varepsilon_{\theta\theta})\right] - \frac{E(r,z)\alpha(r,z)}{1-2\upsilon}T(r,z), \tag{13c}$$

$$\sigma_{r,z} = \frac{E(r,z)}{1+\upsilon}\varepsilon_{rz}. \tag{13d}$$

Where $E(r,z)$ and $\alpha(r,z)$ are modulus of elasticity and thermal expansion coefficient, respectively, that are functions of position. It should be noted that the material properties are assumed to be independent of temperature. As the temperature rise in this study isn't too high, this assumption could be reasonable. The cylinder is clamped on its two end edges. Thus mechanical boundary conditions on the upper and lower edges are assumed as

$$u(r,0) = u(r,L) = 0, \tag{14}$$

$$w(r,0) = w(r,L) = 0. \tag{15}$$

Also on the inner and outer surfaces we have

$$\sigma_{rr}(r_i,z) = \sigma_{rr}(r_o,z) = \tau_{rz}(r_i,z) = \tau_{rz}(r_o,z) = 0. \tag{16}$$

2.3 Graded finite element modeling

In order to solve the governing equations the finite element modeling with graded element properties is used. For modeling a continuously non-homogeneous material, the material property function must be discretized according to the size of element mesh. This approximation can provide significant discontinuities. These artificial discontinuities especially in transient and dynamic problems can cause enormous error in the results [16]. Based on these facts the graded finite element is strongly preferable for modeling the present problem.

For modeling the heat transfer problem, an axisymmetric ring element with triangular cross-section is used to discrete the domain. By taking the three nodal values of temperature as the degrees of freedom a linear model can be assumed as [20]

$$T^e(r,z,t) = \left[N^t(r,z)\right]\{q\}^e, \tag{17}$$

where $[N]$ is the matrix of linear interpolation functions and $\{q\}^e$ is the nodal temperature vector of element as

$$\left[N^t(r,z)\right] = \left[N_i^t(r,z)N_j^t(r,z)N_k^t(r,z)\right], \tag{18}$$

$$\{q\}^e = \left\{q_i\ q_j\ q_k\right\}. \tag{19}$$

Additional information is described in the Appendix A.

Variational form of the present problem leads to minimize the following integral

$$I = 1/2 \iiint_V \left[k_r r \left(\frac{\partial T}{\partial r}\right)^2 + k_z r \left(\frac{\partial T}{\partial z}\right)^2 + 2\rho c T \frac{\partial T}{\partial t}\right] \mathrm{d}v + 1/2 \iint_S h(T^2 - 2T_\infty T)\mathrm{d}s, \tag{20}$$

where V is the volume of the cylinder and S is the boundary on which the convective heat loss is specified.

The cylinder is now divided into the finite elements. It should be noted that thermal conductivity in the radial and axial directions, mass density and thermal capacity depend on r and z coordinates in the above integral. The functional I which is the sum of elemental quantities is minimized by using Eq. (20) subjected to the boundary and initial conditions. The graded finite element equations of heat conduction for each element are then derived as

$$\left[k_1^t\right]^e \{q\}^e + \left[k_2^t\right]^e \{q\}^e + \left[k_3^t\right]^e \{\dot{q}\}^e = \{P_T\}^e, \tag{21}$$

where

$$\left[k_1^t\right]^e = 2\pi \iiint_V r[B^t]^T[D^t(r,z)][B^t]\mathrm{d}V, \tag{22}$$

$$\left[k_2^t\right]^e = 2\pi \iint_S h_r \begin{Bmatrix} N_i^t \\ N_j^t \\ 0 \end{Bmatrix} \begin{bmatrix} N_i^t & N_j^t & 0 \end{bmatrix} r\mathrm{d}s, \tag{23}$$

$$\left[k_3^t\right]^e = \iiint_V \rho(r,z)c(r,z)\left[N^t\right]^T\left[N^t\right]\mathrm{d}V, \tag{24}$$

$$\{P_T\}^e = \iint_S h_r T_\infty \left[N^t\right]^T \mathrm{d}s, \tag{25}$$

$$\left[B^t\right] = \begin{bmatrix} \frac{\partial N_i^t}{\partial r} & \frac{\partial N_j^t}{\partial r} & \frac{\partial N_k^t}{\partial r} \\ \frac{\partial N_i^t}{\partial z} & \frac{\partial N_j^t}{\partial z} & \frac{\partial N_k^t}{\partial z} \end{bmatrix}, \tag{26}$$

$$\left[D^t(r,z)\right] = \begin{bmatrix} rk_r(r,z) & 0 \\ 0 & rk_z(r,z) \end{bmatrix}. \tag{27}$$

The mass density $\rho(r,z)$, conduction coefficient $k(r,z)$ and heat capacity $c(r,z)$ are in general functions of position as well as mechanical properties. Therefore in the graded finite element, their distributions should be assigned into the elemental formulation. For finding the characteristic matrices the integral must be taken over the elemental volume with considering distribution function of material properties through each element. Their distribution functions are given as

$$\rho(r,z)c(r,z) = (\rho c)_{c1}\, V_{c1}(r,z) + (\rho c)_{c2}\, V_{c2}(r,z) + (\rho c)_{m1}\, V_{m1}(r,z) + (\rho c)_{m2}\, V_{m2}(r,z), \tag{28}$$

$$k(r,z) = k_{c1}V_{c1}(r,z) + k_{c2}V_{c2}(r,z) + k_{m1}V_{m1}(r,z) + k_{m2}V_{m2}(r,z). \tag{29}$$

Now by assembling the element matrices, the global matrix equation for the structure can be obtained as

$$\left[K_3^t\right]\left\{\dot{Q}\right\} + \left[K^t\right]\{Q\} = \{P_T\}, \tag{30}$$

where $\{Q\}$ is the vector of nodal temperature of the cylinder and also

$$\left[K_3^t\right] = \sum_{e=1}^{M} \left[k_3^t\right]^e, \tag{31}$$

$$\left[K^t\right] = \sum_{e=1}^{M} \left[k_1^t\right]^e + \left[k_2^t\right]^e, \tag{32}$$

$$\{P_T\} = \sum_{e=1}^{M} \{P_T\}^e, \tag{33}$$

where M is the number of elements.

For thermoelasticity problem axisymmetric elements are also used. Using the triangular shape of element with the nodes i, j, k and defining the nodal displacements as

$$\{a_i(t)\}^e = \begin{Bmatrix} u_i(t) \\ w_i(t) \end{Bmatrix}. \tag{34}$$

A linear polynomial can be used to define uniquely the displacement within the element. Then the displacement field is

$$\begin{Bmatrix} u(r,z,t) \\ w(r,z,t) \end{Bmatrix} = \left[N^s(r,z)\right] \{a(t)\}^e, \tag{35}$$

where $\left[N^s(r,z)\right]$ is the matrix of linear interpolation functions and $\{a(t)\}^e$ is the nodal displacement vector of each element that their components are given in the Appendix A.

The strain-displacement relations can be written as

$$\begin{Bmatrix} \varepsilon_{rr} \\ \varepsilon_{\theta\theta} \\ \varepsilon_{\theta z} \\ \varepsilon_{rz} \end{Bmatrix} = \begin{bmatrix} \partial/\partial r & 0 \\ 1/r & 0 \\ 0 & \partial/\partial z \\ \frac{1}{2}\partial/\partial z & \frac{1}{2}\partial/\partial r \end{bmatrix} \begin{Bmatrix} u \\ w \end{Bmatrix}, \tag{36}$$

or

$$\{\varepsilon\} = [L]\{u\}. \tag{37}$$

Using the displacement functions defined by Eqs. (38) and (40) have

$$\{\varepsilon\} = \left[B^s\right]\{a\}^e, \tag{38}$$

where

$$\left[B^s\right] = [L]\left[N^s\right]. \tag{39}$$

The components of matrices are given in the Appendix A.

The constitutive equations can be written as

$$\{\sigma\} = \left[D^s(r,z)\right](\{\varepsilon\} - \{\varepsilon_T\}), \tag{40}$$

where $\left[D^s(r,z)\right]$ is the matrix of coefficients of elasticity described in the Appendix A. Also the thermal strain is

$$\{\varepsilon_T\} = \alpha(r,z)\Delta T(r,z,t) \begin{Bmatrix} 1 \\ 1 \\ 1 \\ 0 \end{Bmatrix}, \tag{41}$$

where ΔT is the temperature rise in an element.

The strain energy of a linear elastic body is defined as

$$\pi = \frac{1}{2} \iiint_V \{\varepsilon\}^T \{\sigma\} \, \mathrm{d}V, \tag{42}$$

where V is the volume of the body. By using the stress–strain relations the strain energy for each element can be expressed as

$$\pi^e = \frac{1}{2} \iiint_{V^e} \{\varepsilon\}^T \left[D^s\right] \{\varepsilon\} \, \mathrm{d}V - \iiint_{V^e} \{\varepsilon\}^T \left[D^s\right] \{\varepsilon_T\} \, \mathrm{d}V^e. \tag{43}$$

As the work done by the external forces is zero, the potential energy for each element can be expressed as

$$\pi_p^e = \frac{1}{2} \iiint_{V^e} \{\varepsilon\}^T \left[D^s\right] (\{\varepsilon\} - 2\{\varepsilon_T\}) \, \mathrm{d}V^e. \tag{44}$$

Then the potential energy of the body is

$$\pi_p = \sum_{e=1}^{M} \pi_p^e. \tag{45}$$

By substituting Eqs. (41)–(44) into Eq. (47) and summing up, we have

$$\begin{aligned} \pi_p = \frac{1}{2} \{\tilde{a}\}^T & \left[\sum_{e=1}^{M} \iiint_{V^e} \left[B^s(r,z)\right]^T \left[D^s(r,z)\right] \left[B^s(r,z)\right] \mathrm{d}V^s \right] \{\tilde{a}\} \\ & - \{\tilde{a}\}^T \left[\sum_{e=1}^{M} \iiint_{V^e} \left[B^s(r,z)\right]^T \left[D^s(r,z)\right] \{\varepsilon_T\} \, \mathrm{d}V^s \right], \end{aligned} \tag{46}$$

where $\{\tilde{a}\}$ is the vector of nodal displacements of the entire structure.

Now applying the principle of minimum potential energy as

$$\frac{\partial \pi_p}{\partial \{\tilde{a}\}} = 0, \tag{47}$$

the desired equilibrium equations of the overall structure can be expressed as

$$\left(\sum_{e=1}^{M} \left[k^s\right]^e \right) \{\tilde{a}\} = \sum_{e=1}^{M} \{F_T\}^e, \tag{48}$$

or

$$\left[K^s\right] \{\tilde{a}\} = F_T, \tag{49}$$

where the characteristic matrices are given as

$$\left[k^e\right] = \iiint_{V^e} \left[B^s(r,z)\right]^T \left[D^s(r,z)\right] \left[B^s(r,z)\right] \mathrm{d}V^e. \tag{50}$$

Also the load vector caused by temperature can be evaluated as

$$\{F_T\}^e = \iiint_{V^e} \left[B^s(r,z)\right]^T \left[D^s(r,z)\right] \{\varepsilon_T\} \, \mathrm{d}V^s, \tag{51}$$

where the components of $\left[D^s(r,z)\right]$ could be explicit functions describing the actual material property gradient in which modulus of elasticity, $E(r,z)$, is determined at each point through the element using distribution function of this property based on the rule of mixtures as

$$E(r,z) = E_{c1}V_{c1}(r,z) + E_{c2}V_{c2}(r,z) + E_{m1}V_{m1}(r,z) + E_{m2}V_{m2}(r,z), \tag{52}$$

Also the thermal expansion is

$$\alpha(r,z) = \alpha_{c1}V_{c1}(r,z) + \alpha_{c2}V_{c2}(r,z) + \alpha_{m1}V_{m1}(r,z) + \alpha_{m2}V_{m2}(r,z). \tag{53}$$

After assembling the element characteristic matrices and vectors, the boundary conditions are satisfied. As the variational approach is used for deriving the system equations, the natural boundary conditions are implicitly satisfied during solution process. Thus the essential boundary conditions must be applied to Eq. (49). Several methods are available to incorporating constraints [18]. Multiplying diagonal terms of characteristic matrix by a large number and replacing corresponding nodal loads by modified values yield a solution satisfying boundary conditions. Once the finite elements equations are established, the Crank–Nicolson finite difference method with suitable time step is used to solve the equations.

3 Implementation and validation

To verify the present solution, as the similar works to the present work are few, we use a finite length one-dimensional functionally graded cylinder under steady thermal loading. This problem has been solved semi-analytically in Ref. [12] using series solution. Consider a thick hollow cylinder with simply supported end conditions in which the material distribution in radial direction varies from ceramic (Mullite) at the inner surface to metal (Molybdenum) at the outer surface with a power law function. The geometrical parameters are as: length $L = 5\,\text{m}$, inner radius $r_i = 0.7\,\text{m}$, and outer radius $r_o = 1\,\text{m}$. The internal temperature distribution along z-direction is [12]

$$T(r_i,z) = 200\sin\left(\frac{\pi z}{L}\right), \tag{54}$$

The governing equations can be solved using multi-layer approach. More details are described in the Appendix B.

For solving the mentioned problem by graded finite element method developed here as a transient problem, we suppose that the thermal boundary conditions act as initial condition and the material properties vary in radial direction only. Therefore responses after a long time can be considered as the steady state results. Also we suppose that the material properties vary in radial direction only and the volume fraction exponent and property coefficients are taken as: $n_z = 0, n_r = 5, P_{c1} = P_{c2} = P_c, P_{m1} = P_{m2} = P_m$, where P_c is the material property of inner surface which is considered ceramic and P_m is the material property of metallic outer surface.

Comparison of the results in Fig. 6 and Table 2 show good agreement between two methods. The dimensionless value of temperature distribution through the cylinder is shown in the Fig. 6. Also dimensionless values of temperature, radial displacement, radial stress, and tangential stress in a specified point are compared in Table 2.

In this table E_o and α_o are reference values of Young's modulus and thermal expansion coefficients of the functionally graded materials. T_o is reference temperature of the functionally graded circular hollow cylinder.

4 Numerical results and discussion

A thick hollow cylinder of inner radius $r_i = 1\,\text{m}$, outer radius $r_o = 1.5\,\text{m}$ and length $L = 1\,\text{m}$, made of functionally graded material with two-dimensional gradation of distribution profile is investigated. Constituent materials are two distinct ceramics and two distinct metals denoted in Table 1. Volume fraction of materials is distributed according to Eqs. (1)–(4). Responses for some different powers of material composition profile,

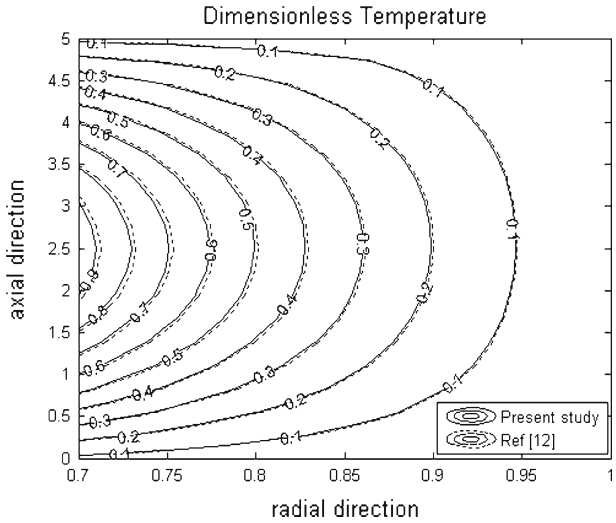

Fig. 6 Comparison of the temperature distribution using GFEM and multi-layer method

Table 2 Comparison of the results between GFEM and multi-layer method

$r/r_o = 0.85, z/r_o = 2.5$	Present study	Ref. [12]
T/T_0	0.336	0.333
$u/\alpha_0 T_0 r_o$	0.422	0.418
$\sigma_r/\alpha_0 E_0 r_o$	−0.611	−0.605
$\sigma_\theta/\alpha_0 E_0 r_o$	0.428	0.423

n_r and n_z are compared. Thermal loading and boundary conditions are

$$\text{at} \quad r = r_i \quad T_i(z,t) = 25 + 100(1 - e^{c_0 t})\sin(\pi z), \tag{55a}$$

$$\text{at} \quad r = r_o \quad k_r \frac{\partial T(r_o, z)}{\partial r} + h_o(T - T_\infty) = 0, \tag{55b}$$

$$\text{at} \quad z = 0 \quad k_z \frac{\partial T(r, 0)}{\partial z} + h_b(T - T_\infty) = 0, \tag{55c}$$

$$\text{at} \quad z = 1 \quad k_z \frac{\partial T(r, L)}{\partial z} + h_u(T - T_\infty) = 0, \tag{55d}$$

$$\text{at} \quad t = 0 \quad T(r, z, 0) = 25°\text{C}, \tag{55e}$$

where, $h_o = h_b = h_u = 100$ W/m^{2}K, $T_\infty = 25°$C and $c_0 = -2$.

In the following figures a cylinder with variation of volume fraction and material properties in two directions is considered. Figs. 7 and 8 show the temperature distribution through the cylinder at different times. Power law exponent of material distribution profile in radial and axial directions are the same, i.e. $n_r = n_z = 2$.

Variations of temperature with time in two different points near the upper and lower edges of the cylinder are illustrated in Fig. 9. The power law exponent in the radial direction is constant, but in the axial direction it varies. Also the time response for a homogeneous cylinder ($n_r = n_z = 0$) is presented in this figure. It is clear that the time responses are strongly affected by material distribution tailoring.

The same results are plotted for two different points near the inner and outer surfaces in Fig. 10.

In order to have a more clear observation, distributions of temperature through the cylinder at different specific times are illustrated in Figs. 11 and 12 for various material compositions. The thermal boundary conditions are as Eqs. (55) in these plots.

It is evident from these figures that both of the amplitude and time delay of the responses are strongly affected by the material distribution powers n_r and n_z.

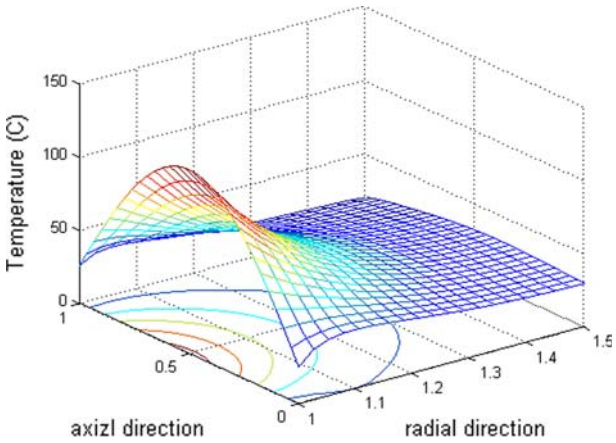

Fig. 7 Temperature distribution through the cylinder after 100 s

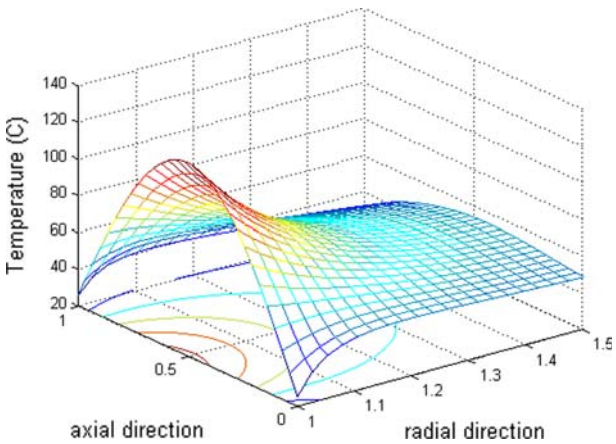

Fig. 8 Temperature distribution through the cylinder after 2,000 s

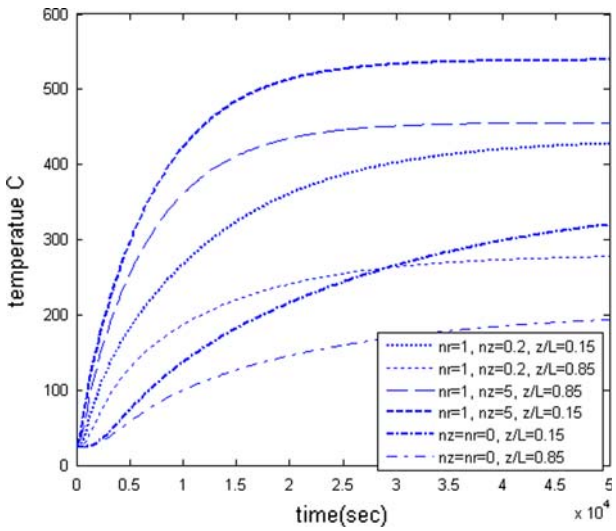

Fig. 9 Transient temperature at points near the upper and lower edges for different material distributions

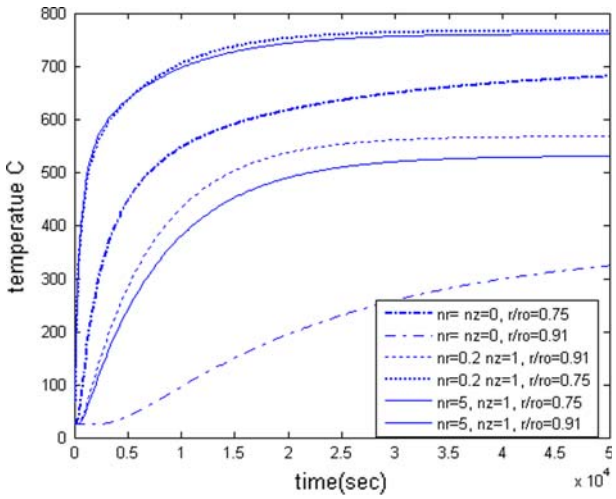

Fig. 10 Transient temperature at points near the inner and outer surfaces for different material distributions

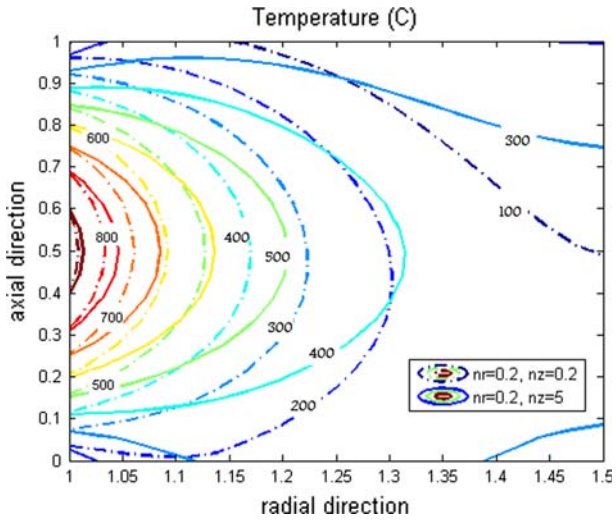

Fig. 11 Temperature distribution through the 2D-FGM cylinder for different power law exponents in the axial direction after 100 s

Distributions of components of displacement caused by thermal loading for different material distribution profiles after 2,000 s are shown in the Figs. 13, 14, 15 and 16. The zero exponents ($n_r = n_z = 0$) means the case of homogeneous material.

In order to observe the stress distributions and variation of thermal stresses with time in the homogeneous cylinder, radial stress distribution through the cylinder in different times after loading are presented in Figs. 17, 18 and 19.

The same results are plotted for 1D FGM cylinder with different material distribution profiles in Figs. 20, 21 and 22. In these figures the axial power law is zero ($n_z = 0$) and the material is graded in radial direction only.

Radial stress distribution for different power law exponents through a 2D-FGM cylinder are shown in Figs. 23, 24, 25, 26 and 27.

Also the distributions of axial and hoop stresses through the cylinder in different times after loading are presented in Figs. 28, 29, 30, 31, 32, 33, 34 and 35 for different power law exponents of material distribution function.

As it is mentioned before, stress distributions in two directions are strongly influenced by the material composition profile. In other words, the time response, the maximum amplitude and the uniformity of stress

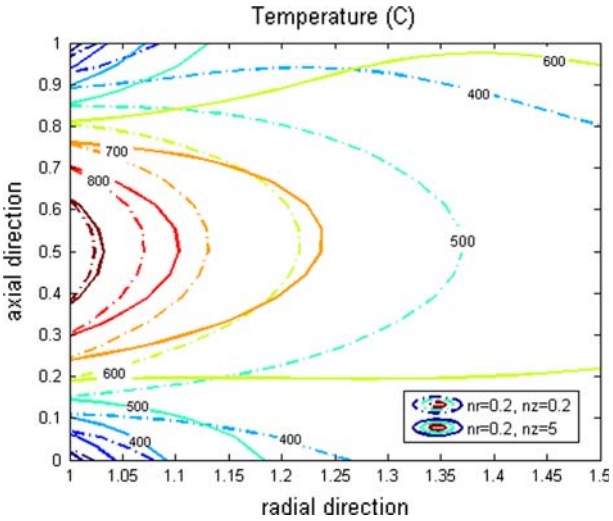

Fig. 12 Temperature distribution through the 2D-FGM cylinder for different power law exponents in the axial direction after 900 s

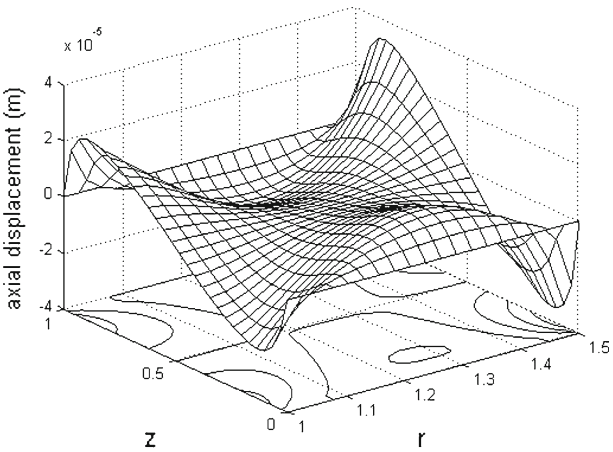

Fig. 13 Axial displacement distribution through the cylinder at $t = 3{,}000$ s for $n_r = n_z = 0$

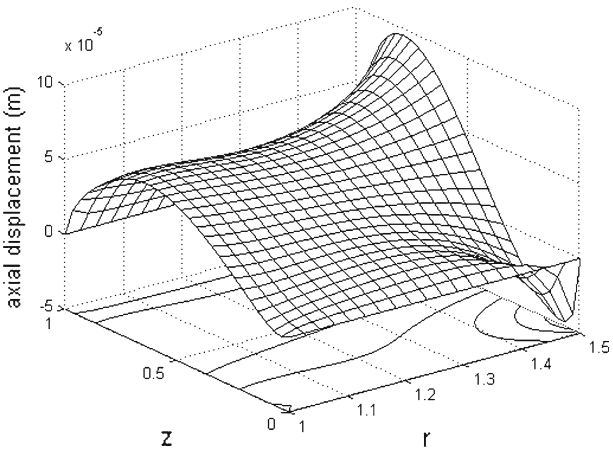

Fig. 14 Axial displacement distribution through the cylinder at $t = 3{,}000$ s for $n_r = n_z = 3$

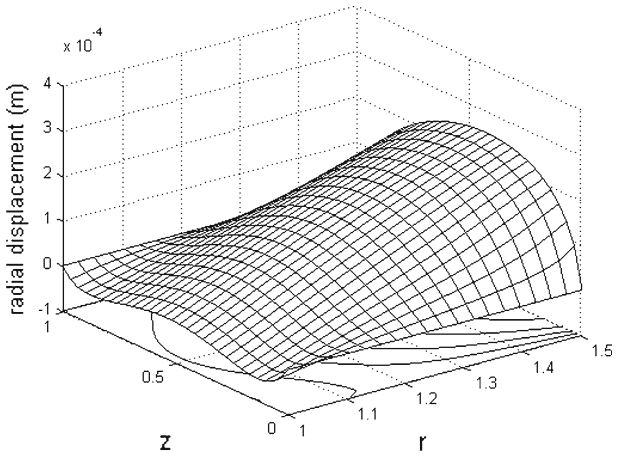

Fig. 15 Radial displacement distribution through the cylinder at $t = 3{,}000\,\mathrm{s}$ for $n_r = n_z = 0$

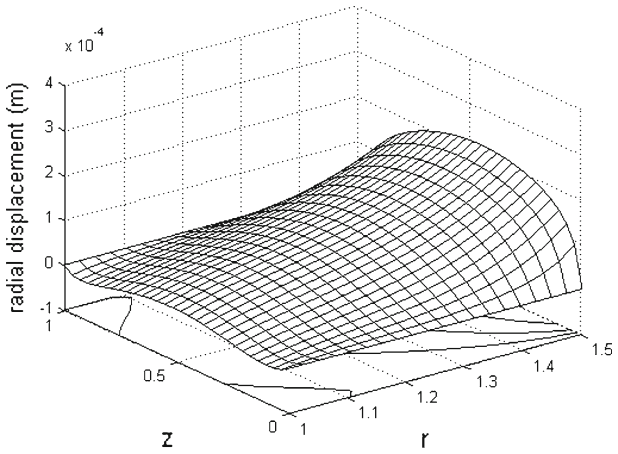

Fig. 16 Radial displacement distribution through the cylinder at $t = 3{,}000\,\mathrm{s}$ for $n_r = n_z = 3$

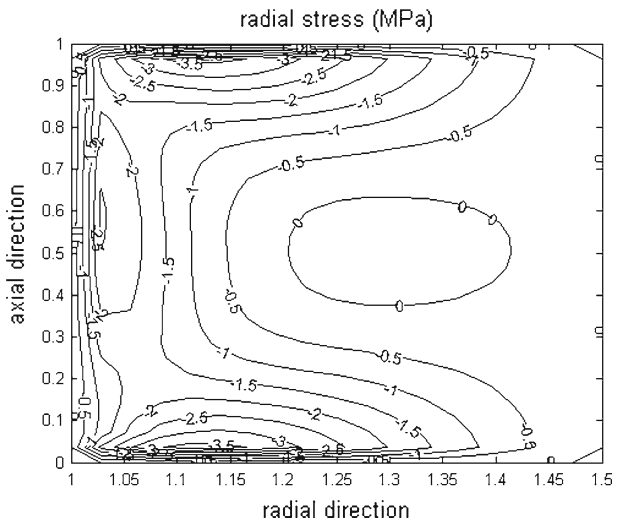

Fig. 17 Radial stress distribution through the cylinder at $t = 30\,\mathrm{s}$ for $n_r = n_z = 0$

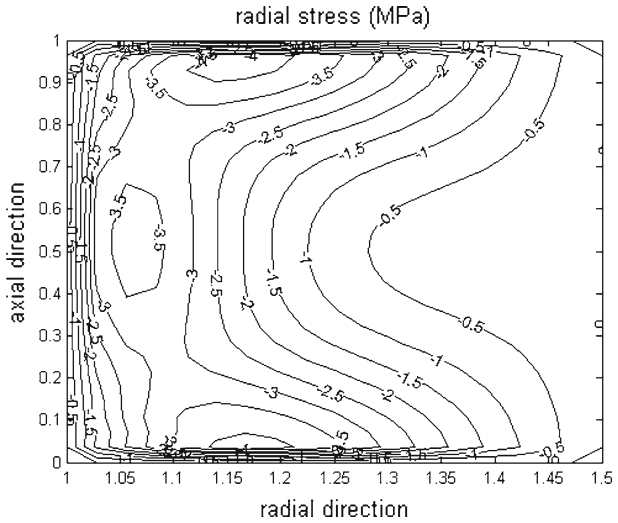

Fig. 18 Radial stress distribution through the cylinder at $t = 1{,}000\,\text{s}$ for $n_r = n_z = 0$

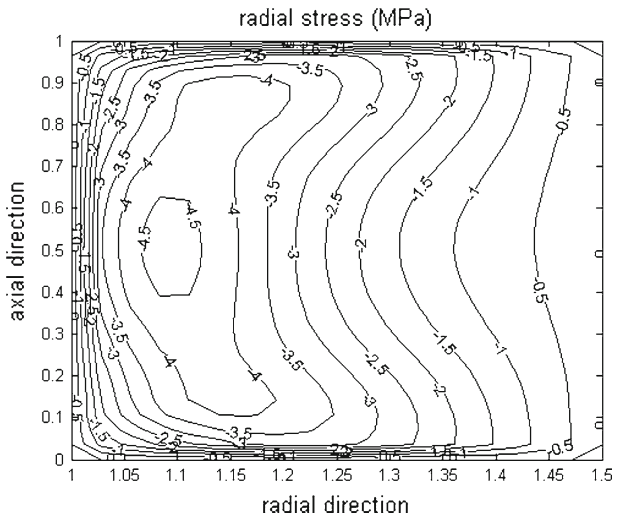

Fig. 19 Radial stress distribution through the cylinder at $t = 3{,}000\,\text{s}$ for $n_r = n_z = 3$

distributions through the cylinder can be modified to a required manner by selecting appropriate material distribution profile. It can be seen that variation of material distribution in two directions leads to a more flexible and desirable design which is very useful in optimization problems.

It should be noted that although the manufacturing of multidimensional FGM may seem to be costly or difficult, but it should be noted that while these technologies are relatively new, processes such as three-dimensional printing (3DP$^{\text{TM}}$) and Laser Engineering Net Shaping (LENS$^{(\text{R})}$) can currently produce FGMs with relatively arbitrary three-dimensional grading [21]. With further refinement FGM manufacturing methods may provide the designers with more control of the composition profile of functionally graded components with reasonable cost.

5 Conclusion

Thermal stresses in a two-dimensional functionally graded cylinder with finite length under transient thermal loading has been studied. For modeling and simulation of governing equations graded finite element method was used that has some advantages to conventional finite element method. The transient responses of 2D-FGM

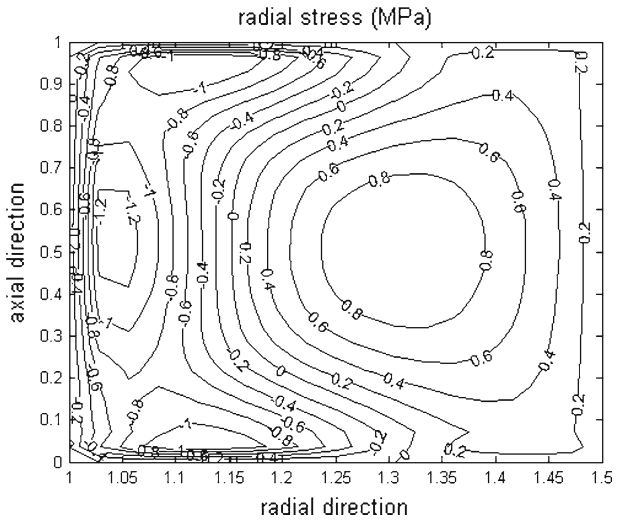

Fig. 20 Radial stress distribution through the cylinder at $t = 30\,\text{s}$ for $n_r = 3, n_z = 0$

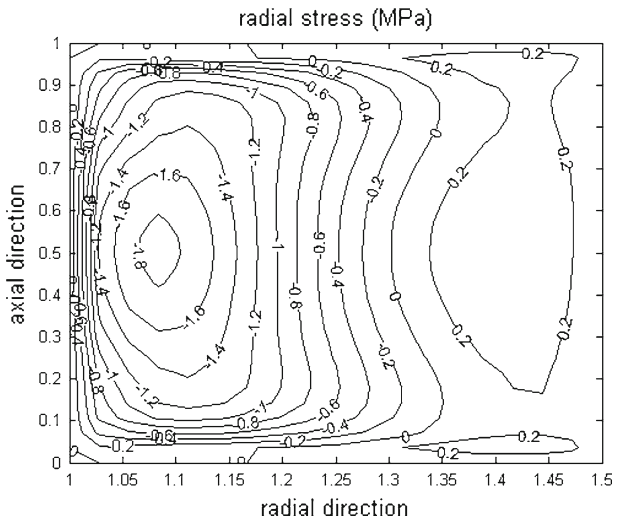

Fig. 21 Radial stress distribution through the cylinder at $t = 1{,}000\,\text{s}$ for $n_r = 3, n_z = 0$

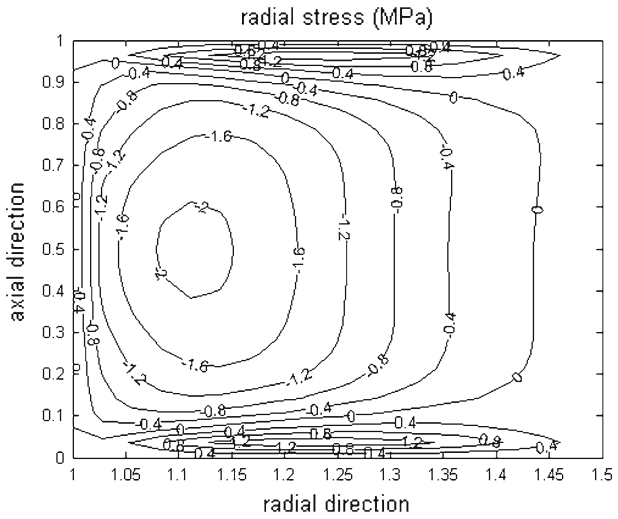

Fig. 22 Radial stress distribution through the cylinder at $t = 3{,}000\,\text{s}$ for $n_r = 3, n_z = 0$

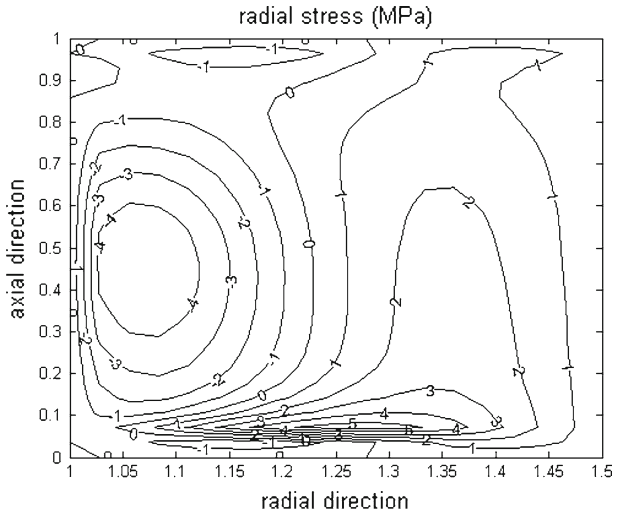

Fig. 23 Radial stress distribution through the cylinder at $t = 30\,\mathrm{s}$ for $n_r = n_z = 3$

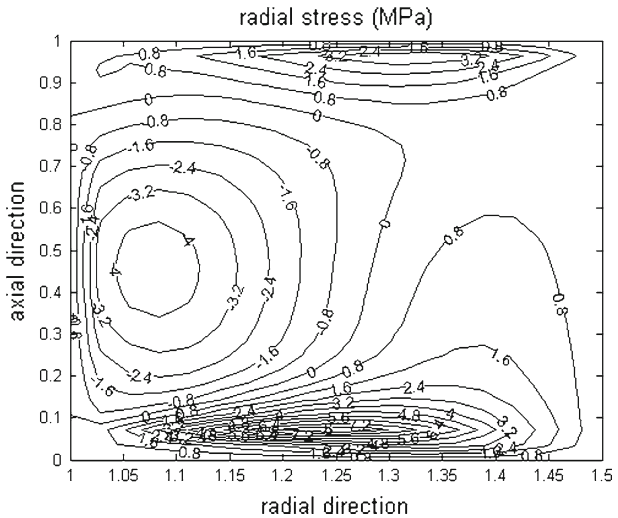

Fig. 24 Radial stress distribution through the cylinder at $t = 3{,}000\,\mathrm{s}$ for $n_r = n_z = 3$

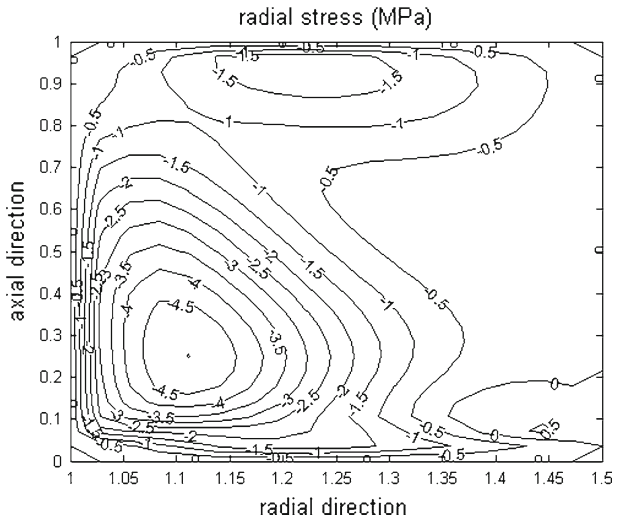

Fig. 25 Radial stress distribution through the cylinder at $t = 30\,\mathrm{s}$ for $n_r = n_z = 0.3$

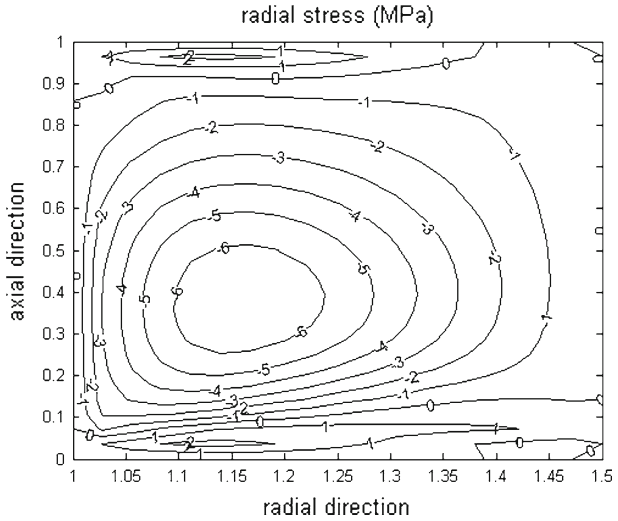

Fig. 26 Radial stress distribution through the cylinder at $t = 1{,}000\,\text{s}$ for $n_r = n_z = 0.3$

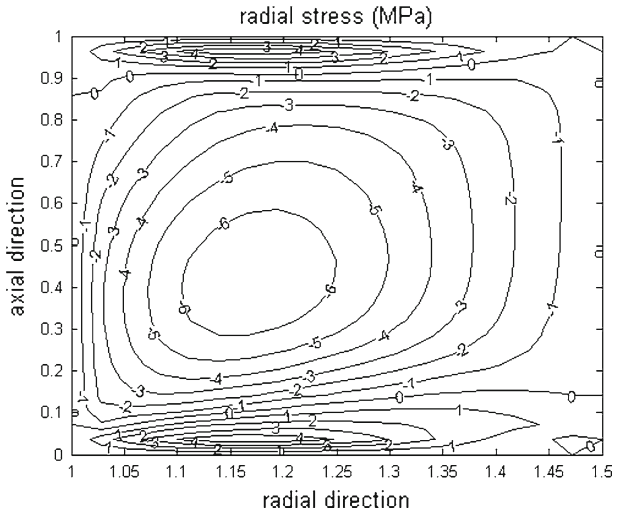

Fig. 27 Radial stress distribution through the cylinder at $t = 3{,}000\,\text{s}$ for $n_r = n_z = 0.3$

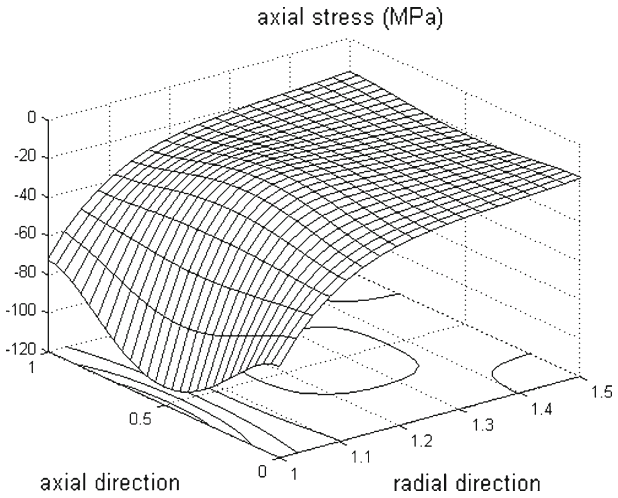

Fig. 28 Axial stress distribution through the cylinder at $t = 30\,\text{s}$ for $n_r = n_z = 0$

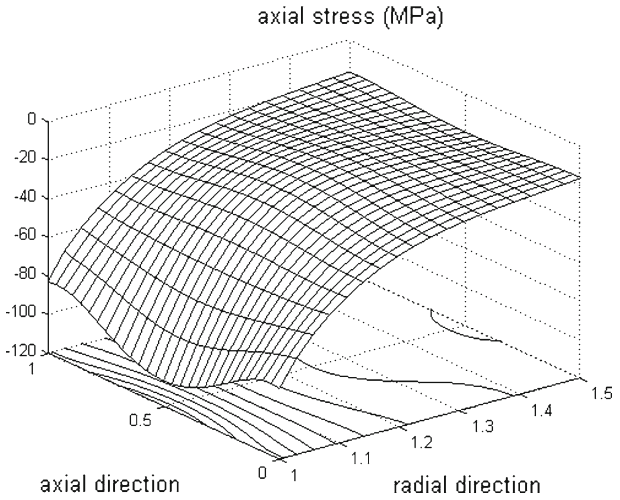

Fig. 29 Axial stress distribution through the cylinder at $t = 3{,}000\,\text{s}$ for $n_r = n_z = 0$

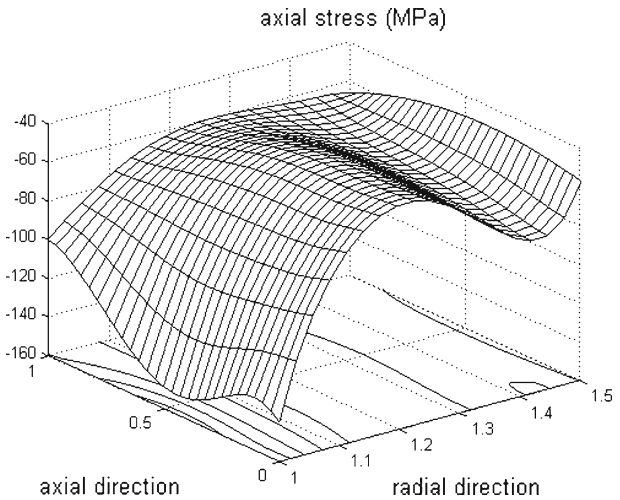

Fig. 30 Axial stress distribution through the cylinder at $t = 30\,\text{s}$ for $n_r = n_z = 3$

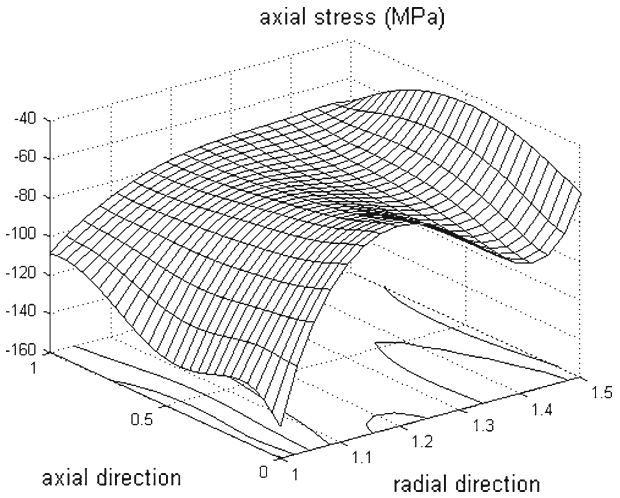

Fig. 31 Axial stress distribution through the cylinder at $t = 3{,}000\,\text{s}$ for $n_r = n_z = 3$

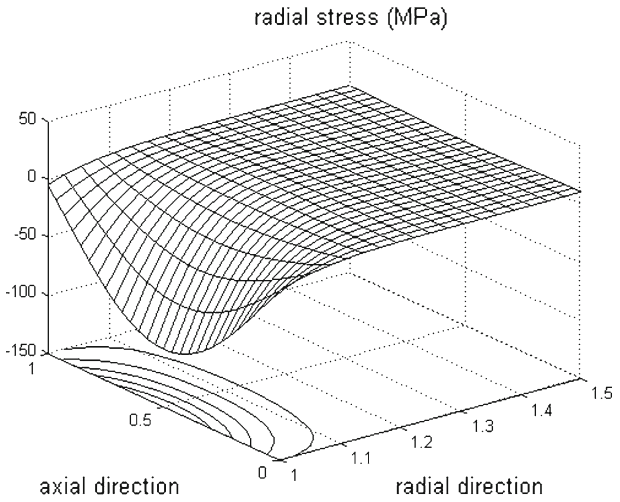

Fig. 32 Hoop stress distribution through the cylinder at $t = 30\,\text{s}$ for $n_r = n_z = 0$

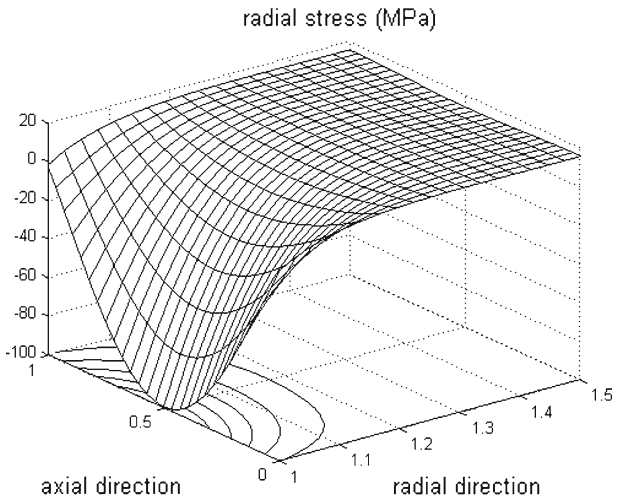

Fig. 33 Hoop stress distribution through the cylinder at $t = 3{,}000\,\text{s}$ for $n_r = n_z = 0$

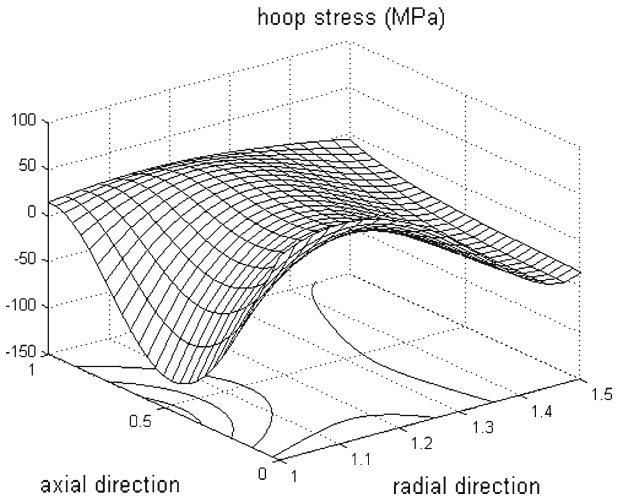

Fig. 34 Hoop stress distribution through the cylinder at $t = 30\,\text{s}$ for $n_r = n_z = 3$

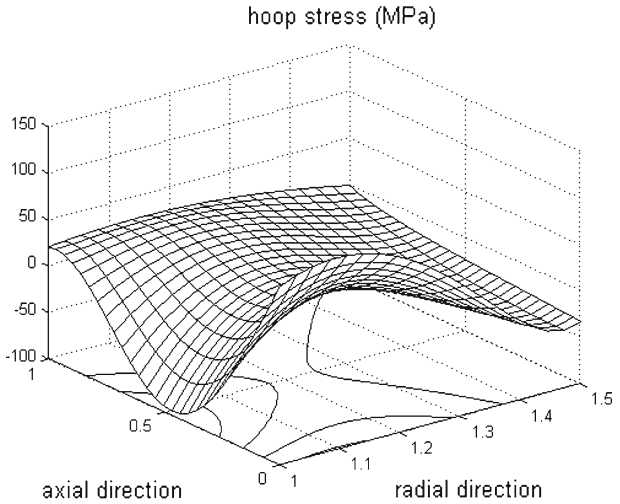

Fig. 35 Hoop stress distribution through the cylinder at $t = 3{,}000$ s for $n_r = n_z = 3$

cylinder are developed and variations of different parameters with volume fraction exponents are obtained. Effects of two-dimensional material distribution on the stress distribution and time responses are considered. Based on the achieved results, 2D-FGMs have a powerful potential for designing and optimization of structures under multi-functional requirements.

Appendix A

The matrix of linear interpolation functions for temperature is

$$\left[N^t(r,z)\right] = \left[\, N_i^t(r,z) \quad N_j^t(r,z) \quad N_k^t(r,z) \,\right] \tag{A1}$$

where subscripts i, j, k are related to three nodes of each element. And its components are

$$N_i^t = \frac{a_i + b_i r + c_i z}{2A}, \tag{A2}$$

$$N_j^t = \frac{a_j + b_j r + c_j z}{2A}, \tag{A3}$$

$$N_k^t = \frac{a_k + b_k r + c_k z}{2A} \tag{A4}$$

where the constants a, b and c are defined in terms of the nodal coordinates as:

$$\begin{aligned} &a_i = r_j z_k - r_k z_j, \quad a_j = r_i z_k - r_k z_i, \quad a_k = r_i z_j - r_j z_i, \\ &b_i = z_j - z_k, \quad b_j = z_k - z_i, \quad b_k = z_i - z_j, \\ &c_i = r_j - r_k, \quad c_j = r_k - r_i, \quad c_k = r_i - r_j. \end{aligned} \tag{A5}$$

And A is the area of the element given by

$$A = 1/2(r_i z_j + r_j z_k + r_i z_k - r_k z_j). \tag{A6}$$

Vector of nodal temperature (degrees of freedom) is

$$\{q\}^e = \begin{Bmatrix} T_i \\ T_j \\ T_k \end{Bmatrix} \tag{A7}$$

The matrix of linear interpolation functions for displacements is

$$\left[N^s\right] = \begin{bmatrix} N_i & 0 & N_j & 0 & N_k & 0 \\ 0 & N_i & 0 & N_j & 0 & N_k \end{bmatrix}. \tag{A8}$$

Where its components are:

$$N_i = \frac{a_i + b_i r + c_i z}{2A}, \tag{A9}$$

$$N_j = \frac{a_j + b_j r + c_j z}{2A}, \tag{A10}$$

$$N_k = \frac{a_k + b_k r + c_k z}{2A} \tag{A11}$$

$$A = 1/2(r_i z_j + r_j z_k + r_i z_k - r_k z_j) \tag{A12}$$

The constants a, b and c are defined in terms of the nodal coordinates and A is the area of the element.

Vector of nodal displacements (degrees of freedom) is:

$$\{a(t)\}^e = \begin{Bmatrix} u_i \\ w_i \\ u_j \\ w_j \\ u_k \\ w_k \end{Bmatrix} \tag{A13}$$

where subscripts i, j, k are related to three nodes of each element.

Also have:

$$\left[B^s\right] = \frac{1}{2A} \begin{bmatrix} b_i & 0 & b_j & 0 & b_k & 0 \\ N_i/r & 0 & N_j/r & 0 & N_k/r & 0 \\ 0 & c_i & 0 & c_j & 0 & c_k \\ c_i & b_i & c_j & b_j & c_k & b_k \end{bmatrix} \tag{A14}$$

$$\left[D^s\right] = \frac{E(r,z)}{(1+\nu)+(1-2\nu)} \begin{bmatrix} 1-\nu & \nu & \nu & 0 \\ \nu & 1-\nu & \nu & 0 \\ \nu & \nu & 1-\nu & 0 \\ 0 & 0 & 0 & \frac{1-2\nu}{2} \end{bmatrix}. \tag{A15}$$

Appendix B

The boundary conditions on the inner and outer surfaces of the cylinder are taken as:

$$\sigma_r^1(r_i, z) = P_i(z), \quad \tau_{rz}^1(r_i, z) = 0 \tag{B1}$$

$$\sigma_r^m(r_o, z) = 0, \quad \tau_{rz}^m(r_o, z) = 0 \tag{B2}$$

where the superscripts 1 and m denotes the inner and outer layers.

And on the top and the bottom end are assumed:

$$u^i(r, 0) = \sigma_z^i(r, 0) = \tau_{rz}^i(r, 0) = 0, \quad i = 1, 2, \ldots, m \tag{B3}$$

$$u^i(r, L) = 0, \sigma_z^i(r, L) = \tau_{rz}^i(r, L) = 0, \quad i = 1, 2, \ldots, m \tag{B4}$$

where superscript i denotes the number of layer.

The continuity conditions to be enforced at any interface between two layers are written as:

$$\begin{aligned} &\sigma_r^{i-1}(r_i, z) = \sigma^i(r_i, z), \\ &\tau_{rz}^{i-1}(r_i, z) = \tau_{rz}^i(r_i, z), \quad i = 2, 3, \ldots, m-1 \end{aligned} \tag{B5}$$

The solution of governing equations for each layer can be expressed as the following sinusoidal series solution that satisfies the boundary conditions [12]:

$$u(r,z) = \sum_{n=1}^{\infty} \varphi_n(r) \sin\left(\frac{n\pi z}{L}\right) \tag{B6}$$

$$w(r,z) = \sum_{n=1}^{\infty} \psi_n(r) \sin\left(\frac{n\pi z}{L}\right). \tag{B7}$$

Substituting above series in the governing equations and applying boundary conditions and continuity conditions the unknown coefficients, $\varphi_n(r)$ and $\psi_n(r)$, can be found.

References

1. Koizumi, M.: The concept of FGM, ceramic transaction, functionally graded materials **34**, 3–10 (1993)
2. Kim, K.S., Noda, N.: Green's function approach to unsteady thermal stresses in an infinite hollow cylinder of functionally graded material. Acta Mech. **156**, 145–161 (2002)
3. Jin, Z.H.: An asymptotic solution of temperature field in a strip of a functionally graded material, Int Common strip of a functionally graded material. Int. Common Heat Mass Trans. **29**(7), 887–895 (2002)
4. Shao, Z.S., Wang, T.J., Ang, K.K.: Transient thermomechanical analysis of functionally graded hollow circular cylinders. J. Therm. Stress **30**, 81–104 (2007)
5. Awaji, H., Sivakuman, R.: Temperature and stress distributions in a hollow cylinder of functionally graded material: the case of temperature- dependent material properties. J. Am. Ceram. Soc. **84**, 059–1065 (2001)
6. Sladek, J., Sladek, V., Zhang, Ch.: Transient heat conduction analysis in functionally graded materials by the meshless local boundary integral equation method. Comput. Mater. Sci. **28**, 494–504 (2003)
7. Shao, Z.S., Ma, G.W.: Thermo-mechanical stresses in functionally graded circular hollow cylinder with linearly increasing boundary temperature. Compos. Struct. **83**(3), 259–265 (2008)
8. Chen, B., Tong, L.: Sensivity analysis of heat conduction for functionally graded materials. Mater Des. **25**, 663–672 (2004)
9. Wang, B.L., Mai, Y.W., Zhang, X.H.: Thermal shock resistance of functionally graded materials. Acta Mater. **52**, 4961–4972 (2004)
10. Wang, B.L., Tian, Z.H.: Application of finite element–finite difference method to the determination of transient temperature field in functionally graded materials. Finite Elem. Anal. Des. **41**, 335–349 (2005)
11. Hosseini, M., Akhlaghi, M., Shakeri, M.: Dynamic response and radial wave propagations of functionally graded thick hollow cylinder. Int. J. Comput. Aided Eng. Softw. **24**(3) (2007)
12. Shao, Z.S.: Mechanical and thermal stresses of a functionally graded circular hollow cylinder with finite length. Int. J. Press. Vessels Piping **82**, 155–163 (2005)
13. Nemat-Alla, M.: Reduction of thermal stresses by developing twodimensional functionally graded materials. Int. J. Solids Struct. **40**(26), 7339 (2003)
14. Abudi, J., Pindera, M.-J.: Thermoelastic theory for the response of materials functionally graded in two directions. Int. J. Solids Struct. **33**(7), 931–966 (1996)
15. Cho, J.R., Ha, D.Y.: Optimal tailoring of 2D volume-fraction distributionsfor heat-resisting functionally graded materials using FDM. Comput. Method Appl. Mech. Eng. **191**(29–30), 3195–3211 (2002)
16. Santare, M.H., Lambros, J.: Use of a graded finite element to model the behavior of nonhomogeneous materials. J. Appl. Mech. **67**(4), 819–822 (2000)
17. Kim, J.H., Paulino, G.H.: Isoparametric graded finite elements for nonhomogeneous isotropic and orthotropic materials. J. Appl. Mech. **69**(2), 502–514 (2002)
18. Stasa, F.L.: Applied Finite Element Analysis for Engineers. CBS Publishing, New York (1985)
19. Boresi, A.P., Chong, K.P.: Elasticity in Engineering Mechanics, 2nd edn. Wiley, New York (1999)
20. Zienkiewicz, O.C., Taylor, R.L.: The Finite Element Method, 5th edn, VII: Soloid mechanics
21. Goupee, A.J., Vel, S.S.: Two-dimensional optimization of material composition of functionally graded materials using meshless analyses and a genetic algorithm. Comput. Methods Appl. Mech. Eng. **195**, 5926–5948 (2006)